

Research on VFTO Simulation Analysis of 1000 kV GIS Test Circuit Considering Dynamic Arcing Model

Yanze Zhang , Xiaoyue Chen , Han Cui, Junjie Si, Zeyu He, Baoquan Wan, Min Dai, Lei Wang, and Jianben Liu 

Abstract—In the research process of very fast transient overvoltage (VFTO), the accuracy of the switching arc model largely determines the calculation results of VFTO. How to more accurately simulate the arc striking and extinguishing process of the arc during the action of the disconnecter is the key issue in the study of the arc model. In this article, the ATP-EMTP electromagnetic transient program was used to simulate arc damping with a series connection of a fixed-value resistance and a time-varying inductance, and the built-in MODELS module was used for programming to simulate the reignition and extinguishing process of the arc based on the gaseous dielectric theory and the energy balance theory. The model was applied to a 1000 kV gas insulated substation (GIS) test circuit. The relationship between the arc damping and arc voltage and current was analyzed, and the arc reignition law during opening and closing is studied. The arcing law obtained is compared with the experimental results of the existing literature, and the accuracy of the simulation model is verified. Simultaneously, the influence of the opening speed of the disconnecter on VFTO was analyzed by simulation. The results show that when the opening speed is less than 0.7 m/s, the maximum value of VFTO in the test circuit increases with the increase in opening speed. After the VFTO amplitude reaches the maximum and continue to increase the opening speed, the VFTO amplitude decreases. This law is consistent with the experimental results of the existing literature, which proves that the arc model built in this article has a certain engineering application value.

Index Terms—Arc damping, arc striking and arc extinguishing criterion, dynamic arcing model, opening speed of disconnecter, very fast transient overvoltage (VFTO).

Manuscript received 2 March 2022; revised 9 June 2022; accepted 28 June 2022. Date of publication 26 July 2022; date of current version 21 November 2022. Paper 2022-PSEC-0241.R1, presented at the 2021 International Electrical and Energy Conference, Wuhan, China, May 28–30, and approved for publication in the IEEE TRANSACTIONS ON INDUSTRY APPLICATIONS by the Power Systems Engineering Committee of the IEEE Industry Applications Society. This work was supported by the Open Fund of State Key Laboratory of Power Grid Environmental Protection under Grant GYW51202001551. (Corresponding author: Xiaoyue Chen.)

Yanze Zhang, Xiaoyue Chen, Han Cui, and Junjie Si are with the School of Electrical Engineering and Automation, Wuhan University, Wuhan 430072, China (e-mail: 3108496520@qq.com; chenxiaoyue@whu.edu.cn; 2021202070064@whu.edu.cn; sjunjie@whu.edu.cn).

Zeyu He is with State Grid Shaoxing Electric Power Supply Company, Shaoxing 312099, China (e-mail: hzy1995@whu.edu.cn).

Baoquan Wan, Min Dai, Lei Wang, and Jianben Liu are with China Electric Power Research Institute, Beijing 100192, China (e-mail: wanbaoquan@epri.sgcc.com.cn; daimin@epri.sgcc.com.cn; wanglei8@epri.sgcc.com.cn; liujianben@epri.sgcc.com.cn).

Color versions of one or more figures in this article are available at <https://doi.org/10.1109/TIA.2022.3193908>.

Digital Object Identifier 10.1109/TIA.2022.3193908

I. INTRODUCTION

VERY fast transient overvoltage (VFTO) is generated by electromagnetic oscillation caused by switching operation or destructive discharge of disconnecter in gas insulated substation (GIS). Due to the slow action speed of the disconnecter and lacking special arc extinguishing device, multiple restriking of arc reignition and prebreakdown are likely to occur in the process of meeting small currents. The GIS substation has a compact structure, and the electrical distance between the adjacent equipment components is relatively close. The internal voltage-traveling wave produces multiple reflections, forming a steep wavefront overvoltage with a higher amplitude. The initial front edge of the VFTO waveform is in the range of hundreds of nanoseconds, the frequency range is from several thousand hertz to several hundred megahertz, and the overvoltage amplitude can reach 2.0–3.0 p.u. Its waveform and amplitude depend not only on the internal structure of the GIS but also on its external layout [1]–[3].

Due to the limitation of test conditions and measurement methods, simulation calculation plays a very important role in the research of VFTO. Building a complete and accurate transient model will improve the calculation and simulation accuracy of VFTO to a certain extent. Among them, the research on the arc model is particularly critical. From a microscopic point of view, an electric arc is a cluster of particles accompanied by physical and chemical processes of ionization and deionization. During the entire combustion process of the arc, there are a large number of free and defree diffusion and recombination processes, accompanied by complex light and heat energy transfer. The existing arc models can be divided into three categories: physical models, black box models, and parametric models [4]. The most widely used physical arc model is the magnetohydrodynamic model, which follows the laws of thermodynamics, fluid mechanics, and Maxwell's equations, describes the microscopic process of arc development and is mainly used in the design of circuit breakers. The black box model does not consider the complex physical process inside the arc. It uses the correlation among the arc conductance, current, and voltage to describe the circuit characteristics during the arc development process with differential equations, which can directly obtain the dynamic changes of current and voltage during the switching operation transient process. Common black box models include Mayr model and Cassie model [5]. Both of these arc models are based on the energy conservation law. The arc is considered to be a variable resistance. Under the assumption that the arc

shape is cylindrical, the arc is studied on a macroscopic level. Since the basic parameters of the black box model need to be extracted from the experiment, this type of model has a strong dependence on the experiment. The parametric model is to use the volt-ampere characteristics of the arc to equate the arc to a certain circuit element or a combination of several circuit elements. Based on the existing parameter models, through the research on the breakdown voltage of the contact gap of the disconnector of the GIS substation in the former pieces of literature, this article constructs a dynamic arc model based on the dielectric insulating strength recovery characteristics of the fracture. The improved model takes into account the arcing and arc extinguishing conditions, which reflects the dynamic changes of the breakdown voltage and the fracture voltage of the disconnector and provides a more accurate expression for the arc model.

II. ARC MODELING METHOD OF DISCONNECTOR

A. Overview of Arc Damping Model

In engineering calculations, static arc resistance is usually used to simulate arc [6]. In the general computer simulation calculation of VFTO, time-varying resistance is usually used to represent arc. This model describes the resistance change of the switch from the disconnection to the breakdown state. However, it did not take the arc extinguishing process into consideration [7]. Another segmented arc model takes into account the extinguishing phase of the arc [8]. Besides, the prebreakdown stage of the segmented arc model can be improved by hyperbolic functions. On the basis of the above-mentioned segmented arc model, Liu et al. [9] used Mayr's mathematical model to further improve the arc extinguishing stage and proposed an improved dynamic arc model that considers the effect of arc current zero-crossing extinguishing. Liu [10] proposed that an additional inductance can be connected in series with the arc resistance to better simulate the dynamic physical process of the disconnector arc. The arc damping model is simpler than the segmented arc resistance model and more accurate than the static resistance model.

B. Criterion of AC Arc Striking and Extinguishing

For the study of the arc striking and extinguishing process of ac arc, there are usually two corresponding theories: gaseous dielectric theory and energy balance theory [8]. The gaseous dielectric theory believes that the arc striking process is the result of the gap breakdown due to an external electric field. As long as the gap voltage U_d is greater than the breakdown voltage between the gaps U_f , it is considered that an arc occurs between the electrodes. And the extinguishing condition of ac arc is that after the current crosses zero, the recovery strength of the arc gap medium is always higher than the recovery voltage on the arc gap at any time. The energy balance theory believes that the restriking of the arc is not only a simple contact gap breakdown after the current crosses zero but also the rebalance of the energy between the circuit and the arc gap. The arc will only start to extinguish when the injected energy of the arc is less than the

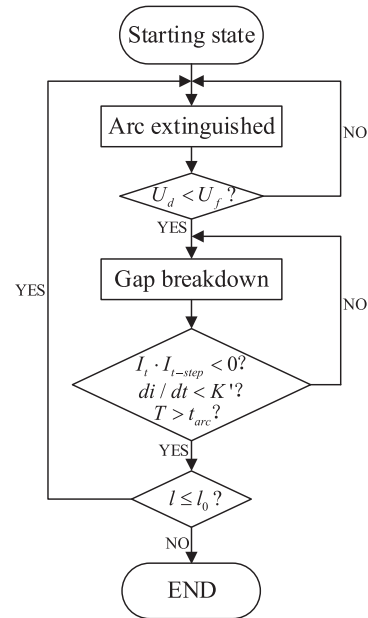


Fig. 1. Criterion of arc restriking and extinguishing in disconnector operation.

lost energy of the arc. When the voltage between the moving and static contacts is greater than the SF₆ breakdown voltage, the gap breaks down and the arc starts to burn. When the arc is extinguished, according to the energy balance theory, if the arc gap input energy is less than the arc gap dissipated energy, the arc energy is reduced and the arc is extinguished. This theory can explain the phenomenon that in the initial stage of breakdown, in spite of the ac high-frequency current crosses zero many times, the arc cannot be extinguished because the energy input to the arc gap is greater than the energy emitted. The arc extinguishing criterion based on the energy balance theory actually needs to meet two conditions at the same time

$$I_t \cdot I_{t\text{-step}} < 0 \quad (1)$$

$$I_t - I_{t\text{-step}} < K. \quad (2)$$

Among them, formula (2) can be described as follows:

$$\lim_{\text{step} \rightarrow 0} \frac{I_t - I_{t\text{-step}}}{\text{step}} = \frac{di}{dt} < Kt. \quad (3)$$

In addition, because the disconnector always has a most suitable arc extinguishing distance when it interrupts the arc, correspondingly, there is the shortest arcing time t_{arc} of the disconnector. If the gaseous dielectric theory is used as the arc reignition criterion and the arc extinguishing criterion adopts the energy balance theory, the process of arc striking and extinguishing during the operation of the disconnector can be represented by the flowchart, as shown in Fig. 1.

In the figure above, l_0 and l , respectively, represent the maximum and actual opening distance between contacts.

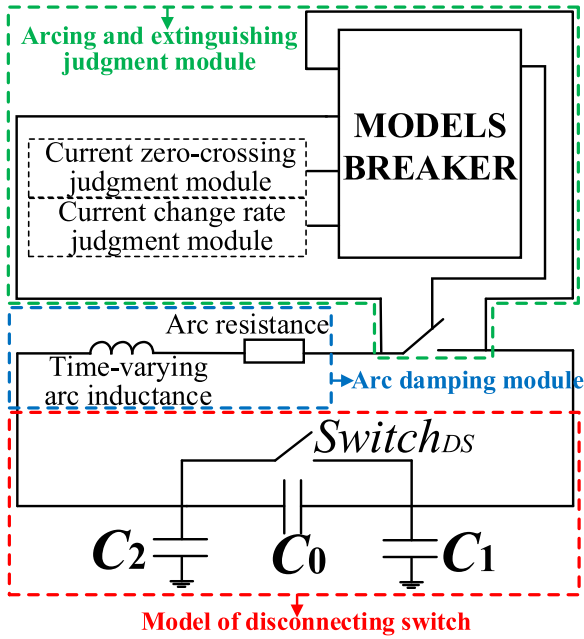


Fig. 2. Schematic diagram of the dynamic arcing model of disconnecting switch.

III. CONSTRUCTION OF THE RESTRIKING ARC MODEL

A. Construction of Arc Damping Model

Most of the existing improvements to the arc model are based on the study of arc damping and use time-controlled switches or voltage-controlled switches to simulate arc breaking. The accuracy of these studies is less than satisfactory and it is difficult to accurately reflect the development process of arcs at different voltage levels. It also did not consider the dielectric insulating strength recovery characteristics of the disconnecter fracture, cannot simulate the competitive relationship between the breakdown voltage of the switch contact gap and the dynamic recovery characteristics of the fracture, and cannot accurately reflect the arc striking and arc extinguishing criterion. One of the reasons for the complex VFTO waveform and the rich spectral components is that the isolation switch may have multiple restriking, such as prebreakdown and reignition during operation, resulting in superimposition of the waveform. Most of the existing arc models are developed around the single breakdown model. Although it can reflect the VFTO amplitude to a certain extent, when the distance between the moving and static contacts of the disconnecter changes over time, it cannot accurately simulate the development of arc during a switch action. Therefore, it is necessary to build the restriking model of the arc in the VFTO simulation circuit to simulate the actual waveform of the VFTO more accurately.

In this article, the arc damping is considered from a more strict point of view. The static arc resistance is generally in the range of 2–5 Ω . Considering that the increase of arc resistance can restrain VFTO, in order to get the VFTO waveform in more serious cases, the arc resistance is 2 Ω . In addition, under the action of high-frequency arc current, the ratio of the voltage drop caused by inductance component to the total voltage drop will increase, so the

inductance characteristics of high-frequency arc channel cannot be ignored. In engineering calculation, the channel inductance can be approximately calculated according to Martin's formula

$$L_{\text{arc}}(t) = 14l. \quad (4)$$

The unit of $L_{\text{arc}}(t)$ is nH; and l is the length of the discharge channel, in cm.

According to the test results of the existing pieces of literature [11], it can be fitted that the relationship between the positive breakdown voltage of the opening and closing operation contact gap and the formation time of the contact gap of 1000 kV GIS test circuit is as follows:

$$U_{r-\text{op}} = 17.1t \quad (5)$$

$$U_{r-\text{cl}} = 1600 - 18.82t \quad (6)$$

where $U_{r-\text{op}}$ and $U_{r-\text{cl}}$ are the breakdown voltage of contact gap in the process of opening and closing, in kV; and t is the formation time of contact gap, in ms. The above formula is based on the following assumptions [12].

- 1) The breakdown voltage of the disconnecter contact gap is proportional to the contact gap distance.
- 2) The contact moves at a constant speed.

It can be concluded that the general equation of the positive breakdown voltage of the contact gap changing with its formation time during the opening and closing process of the disconnecter is as follows:

$$U_{r-\text{op}} = K v_{\text{op}} t \quad (7)$$

$$U_{r-\text{cl}} = K(l_0 - v_{\text{cl}} t) \quad (8)$$

where l_0 is the maximum opening distance of the contact gap of the disconnecter, and v_{op} and v_{cl} are the moving speeds of the disconnecter contact in the process of opening and closing. K represents the positive breakdown voltage per unit length of the contact gap of the disconnecter, and K is a fixed value for a specific disconnecter. According to relevant pieces of literature, the typical value of contact opening distance of disconnecter is 50–70 mm when breakdown occurs. In this article, the value of l_0 is 50 mm. According to the above fitting curve, $K = 32$ kV/mm, average opening speed $v_{\text{op}} = 0.53$ m/s, and average closing speed $v_{\text{cl}} = 0.59$ m/s.

If the contact opening distance reaches the maximum value, the discharge channel length is assumed to be 100 mm. It is approximately considered that the change speed of the discharge channel length with time is equal to the movement speed of the contact

$$l_{\text{op}}(t) = v_{\text{op}} t = 0.107t \quad (9)$$

$$l_{\text{cl}}(t) = l_0 - v_{\text{cl}} t = 10 - 0.118t \quad (10)$$

where $l_{\text{op}}(t)$ and $l_{\text{cl}}(t)$ are the lengths of discharge channel changing with time in the process of opening and closing, respectively, and their values range is 0–10 cm. Substituting $l_{\text{op}}(t)$ and $l_{\text{cl}}(t)$ into Martin's formula to calculate the variation of arc inductance with time in the process of opening and closing

$$L_{\text{arc-op}}(t) = 14l_{\text{op}}(t) = 1.496e^{-3}t \quad (11)$$

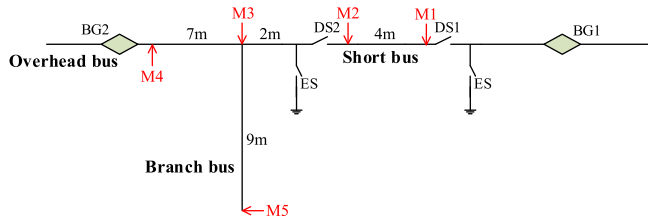


Fig. 3. Layout of a 1000 kV GIS test circuit.

$$L_{\text{arc-cl}}(t) = 14l_{\text{cl}}(t) = 0.14 - 1.65e^{-3}t \quad (12)$$

where $L_{\text{arc-op}}(t)$ and $L_{\text{arc-cl}}(t)$ are the arc inductances in the process of opening and closing, in μH . The unit of t is ms. There is no residual voltage when $t = 0^+$ in the opening process, and the residual voltage at the short bus is -1.0 p.u. when $t = 0^+$ in the closing process. In addition, the length of the shortest line in ultra-high voltage (UHV) test circuit is 2 m, and the wave speed is calculated at 3×10^8 m/s, so the wave propagation time on this section of the line is 6.7 ns. It is defined that the calculated time step should not exceed one-tenth of the shortest wave propagation time. Therefore, 0.5 ns is taken as the simulation step, and the arc current of the disconnector and VFTO of the test circuit under the restriking arc model are calculated. According to the above theories, the schematic diagram of the dynamic arcing model of the disconnector in ATP-EMTP is shown in Fig. 2.

In the above figure, the criterion, as shown in Fig. 1, can be programmed in the MODELS BREAKER module to judge the arc restriking and extinguishing processes.

B. Calculation Model of 1000 kV GIS Test Circuit

The layout of a 1000 kV GIS test circuit is shown in Fig. 3 [13].

Due to the high frequency of VFTO oscillation, the penetration depth of high-frequency electromagnetic wave to good conductors is limited, and the displacement current effect between the conductors is significant, that is, the capacitive reactance between conductors is relatively small, and the inductive reactance is relatively large. Therefore, most components in GIS are represented by lumped parameter capacitance. GIS bus, overhead line, and cable are equivalent by transmission line model. The closed state of the circuit breaker is equivalent to the connected state. The open state of the circuit breaker is simulated by two transmission lines connected in series through capacitors. The simulation of the disconnector is similar to that of the circuit breaker.

IV. VFTO CALCULATION RESULTS AND ANALYSIS

A. Relationship Between Arc Damping and Voltage and Current

According to the above simulation model, taking the closing process as an example, the relationship between arc voltage and current and arc damping in the early stage of the closing operation is shown in Fig. 4.

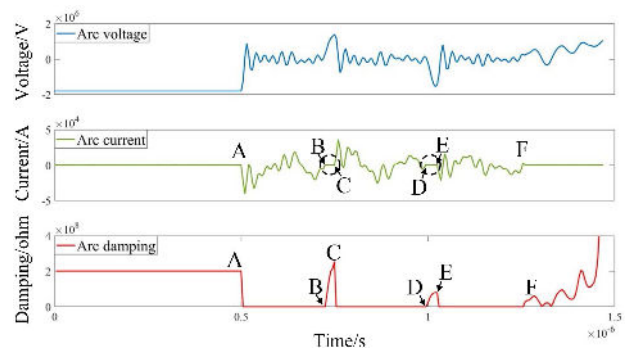


Fig. 4. Relationship between arc voltage and current and arc damping in the early stage of closing operation.

During the simulation period corresponding to this figure, there are three arc ignition and arc extinguishing processes in total, which correspond to A-B-C, C-D-E, and E-F, respectively, in the schematic diagram of arc current and arc damping. Point A is the moment before the arc strikes for the first time. At this time, the current is equal to zero and the arc damping is extremely large. Afterward, the first arcing process began and the arc damping dropped quickly and remained near a small arc resistance. The corresponding arc current at point B is 0, and the current change rate at this point is very small. Point B also meets the limitation of the shortest arc burning time, so the arc is extinguished, and the arc resistance rises sharply to about $300 \text{ M}\Omega$ in a short time. Point C meets the arc striking criterion, the arc reignites, the arc damping quickly drops again, and the second arc extinguishing process is the same as the first. Similarly, the third breakdown occurs at point E. The three segments A-B-C, C-D-E, and E-F in the arc resistance diagram have the same changing law as the segmented resistance arc model, which also proves the correctness of the dynamic arc model from the side.

B. Analysis on the Law of Arc Reignition During Opening and Closing Operation

In addition, the whole process waveform of the contact gap voltage difference and the bus voltage waveform during the opening and closing process of four power frequency cycles (0.08 s) are obtained through simulation. Among them, the contact gap voltage difference curve is shown in Fig. 5.

Known from the picture above, during the opening and closing process, the contact gap voltage difference curve has the outline of the power frequency sinusoidal voltage as a whole. This is because the contact gap voltage is related to the power frequency voltage and the short bus-side residual voltage, which changes with the power frequency sinusoidal voltage. At the same time, since the gaseous dielectric theory is used as the arc striking criterion, the envelope of the contact gap voltage difference curve is the breakdown voltage curve. During the opening operation, the breakdown voltage increases with the increase of the contact opening distance; and during the closing operation, the contact opening distance decreases and the breakdown voltage decreases.

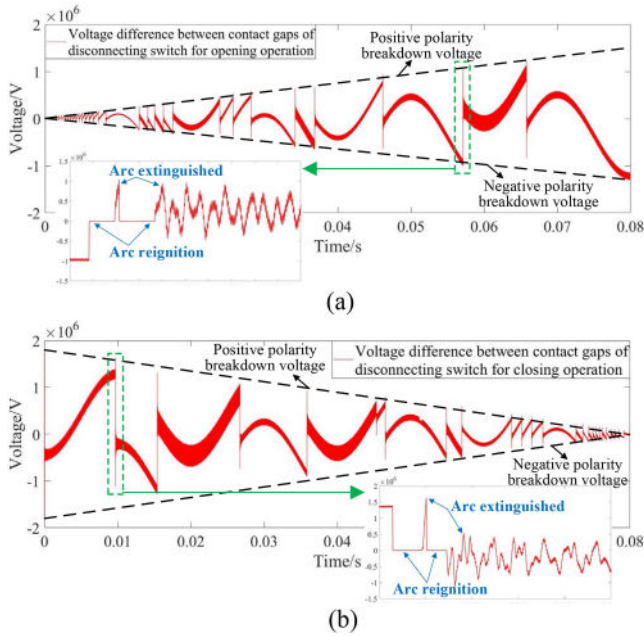


Fig. 5. Contact gap voltage difference curve during opening and closing. (a) Opening operation. (b) Closing operation.

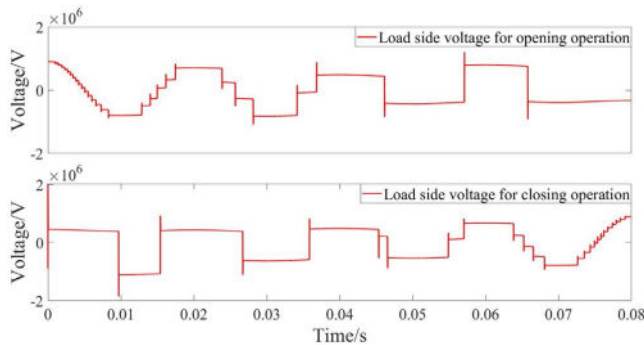


Fig. 6. Relationship between the short bus voltage and the power frequency power supply voltage during the opening process.

It can be seen from Fig. 6 that, during the opening process of the disconnecting switch, as the distance of the contact gap increases, the load-side voltage waveform presents a transition from a sine wave to a step wave. The closing process is just the opposite, and the load-side voltage waveform presents a transition from a step wave to a sine wave.

For the UHV test circuit, as shown in Fig. 3, taking the opening process as an example, when the disconnecting switch DS2 is closed, the voltage on the short bus is the same as the power supply voltage; when DS2 is opened, the short bus is at a floating potential. The floating potential is composed of two components: the first is residual voltage determined by the charge remaining on the short bus, and the second is induced voltage determined by the voltage division between the DS2 fracture capacitance and the short bus-to-ground capacitance. The contact gap voltage is determined by the power frequency power supply voltage and residual voltage. Therefore, the contact gap voltage changes with the power frequency sinusoidal voltage. According to the ac arc striking criterion, when the DS2 contact gap voltage is greater

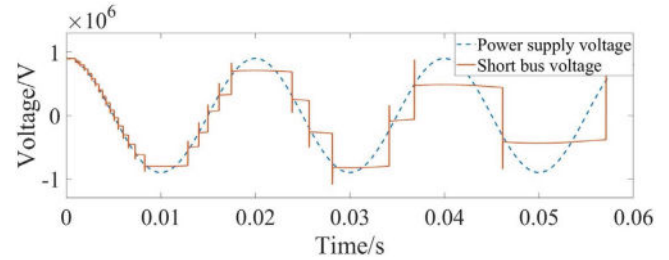


Fig. 7. Load-side voltage waveform during opening and closing.

than the breakdown voltage, the gap is broken down and a high-frequency transient occurs. When the high-frequency transient attenuation process ends, the arc is extinguished, and the residual voltage on the short bus is equal to the instantaneous value of the power frequency voltage of the power supply at the moment of arc extinction. The relationship between the short bus voltage on the load side and the power frequency power supply voltage is shown in Fig. 7.

It can be seen from Fig. 7 that the short bus voltage has an approximate step shape and the outline of the sinusoidal voltage waveform of the power frequency power supply. The transition edge of each step corresponds to a breakdown process, and the narrow pulse corresponding to each transition edge is a high-frequency transient process. At the same time, since the residual voltage of the short bus at the end of each breakdown process is equal to the instantaneous value of the power frequency power supply voltage at the corresponding time, the starting point of each step falls on the power frequency power voltage waveform. It can be seen that the short bus VFTO is actually a superposition of a high-frequency transient on the power frequency power supply voltage. The amplitude of the high-frequency transient itself depends on the magnitude of the arc gap energy when the breakdown occurs. Generally speaking, the larger the contact distance, the greater the gap breakdown voltage, the higher the gap voltage required when the breakdown occurs, and this will result in greater gap energy and high-frequency transient amplitude. At the same time, if the high-frequency transient is superimposed on the peak of the power frequency power supply voltage, the theoretical maximum value of VFTO will be obtained; if it is superimposed on the rising edge of the power frequency voltage, the corresponding VFTO amplitude will decrease. Therefore, the power frequency phase when the breakdown occurs also has a great impact on the VFTO amplitude.

During an opening operation, there will be multiple gap breakdowns and arc extinguishing processes, correspondingly, a series of high-frequency transient processes will occur. When the contact opening distance is increased to the point that the corresponding breakdown voltage will no longer be lower than the gap voltage, the restriking process during the opening operation ends. The residual voltage of the short bus after the last breakdown of the opening process determines the contact gap voltage of the first breakdown during the closing process. Prebreakdown occurs when the contact gap voltage is greater than the breakdown voltage during the closing operation, and

the subsequent arc extinguishing and repeated gap breakdown processes are the same as the opening. As the contact opening distance decreases during the closing process, the breakdown voltage decreases until the DS2 contact is completely closed.

In addition, it is worth noting that for the reignition model, when the closing operation is simulated, breakdown occurs when the power frequency power supply reaches +1.0 p.u. and the residual voltage is -1.0 p.u., and the oscillation overshoot is superimposed on the peak of the power frequency power supply; when simulating the opening operation, the gap breakdown voltage increases as the contact distance increases. Therefore, the maximum value of VFTO usually appears in the later stage of an opening operation; however, it is difficult to ensure that the last breakdown occurs when the distance between the moving and static contacts of DS2 reaches the maximum, and the oscillation overshoot is not necessarily superimposed on the peak value of the sinusoidal power supply; the VFTO of the opening process in the reignition model is lower than the VFTO of the closing process.

Fig. 8 shows the VFTO waveform at the end of the branch bus in the most severe case during the closing and opening simulation of the dynamic arc model. Assuming that the corresponding amplitude of the power frequency voltage is U_0 when the breakdown occurs, the overshoot amplitude of the high-frequency transient oscillation is ΔU . U_0 equals 898 kV and 580 kV while closing and opening, respectively, and ΔU equals 1762 kV and 960 kV, respectively. It can be seen that compared to the closing process, ΔU of the opening process is lower; this is because the contact opening distance does not reach the maximum when the last breakdown occurred, so the gap breakdown voltage is low, and the corresponding contact gap voltage difference is small, which results in a lower overshoot amplitude of the transient oscillation. At the same time, the high-frequency oscillation overshoot is not superimposed on the peak of the power frequency voltage, so U_0 is also relatively small.

From the above analysis, the improvement of the proposed model comparing with the existing ones can be clarified as follows. The physical model is too complex to be used in the engineering calculation of VFTO; the black box model is mostly developed from the Cassie–Mayr model based on the energy balance theory, while its basic parameters are highly dependent on the experiment, which is not conducive to the engineering calculation. The commonly used parametric models cannot accurately simulate the competitive relationship between the gap breakdown voltage and dynamic recovery characteristics of fracture and cannot be reflected in the phenomenon of prebreakdown and multiple reignition of contact gap during one complete action of the disconnecter. The dynamic arcing model established in this article combines the gaseous dielectric theory with the energy balance theory and considers the dynamic change of arc damping with the contact gap distance. The new model cannot only make up for the defects of the parametric model mentioned above but also be easy to implement, which is conducive to the efficient simulation calculation of VFTO in engineering applications.

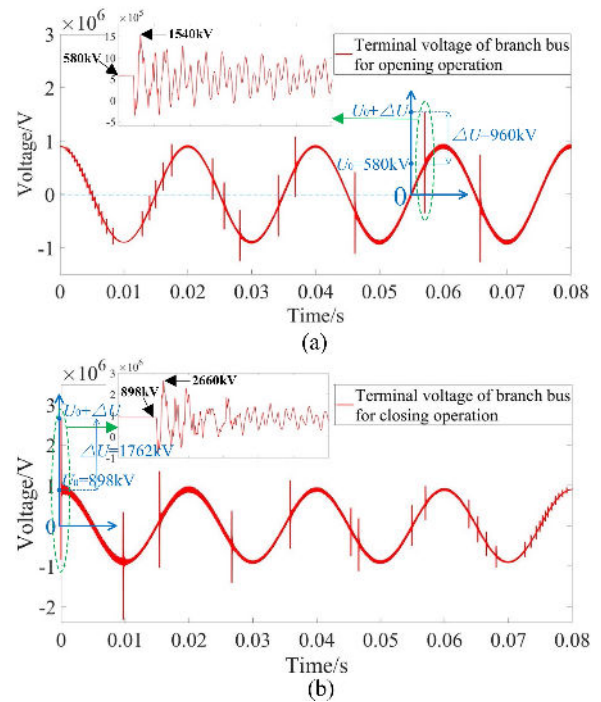


Fig. 8. VFTO waveform at the end of branch bus during the opening and closing of dynamic arc model. (a) Opening operation. (b) Closing operation.

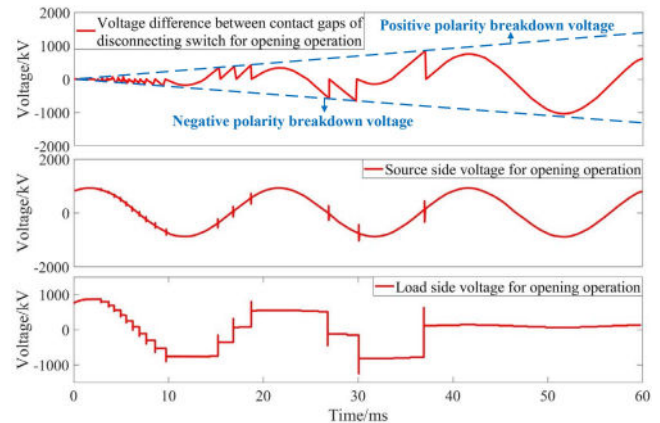


Fig. 9. Experimental results based on the same test circuit in [12].

V. SIMULATION RESULT VERIFICATION

A. VFTO Waveform Comparison

Literature [12] uses the same test circuit to simulate VFTO and obtains the change of the gap recovery voltage and breakdown voltage as well as typical waveforms of the load side and power side of the disconnecting switch during the opening process; the results are shown in Fig. 9. Comparing Figs. 5, 6, and 8 with Fig. 9, we can see that under the simulation conditions of the dynamic arcing in this article, the waveform law of the power side and load side as well as the gap recovery voltage of the test circuit during the opening process is consistent with the typical simulation law in the literature [6]. This also verifies that the dynamic arcing model proposed in this article can accurately

TABLE I
VFTO AMPLITUDE OF BRANCH BUS TERMINAL UNDER DIFFERENT OPENING SPEEDS

$v(\text{m/s})$	0.1	0.2	0.3	0.4	0.5
VFTO(p.u.)	1.21	1.35	1.41	1.50	1.55
$v(\text{m/s})$	0.6	0.7	0.8	0.9	1.0
VFTO(p.u.)	2.55	2.70	2.31	1.90	2.39

reflect the repeated breakdown voltage waveform law of the test circuit during the opening and closing operations of the disconnecting switch.

B. Comparison of the Influence of Opening Speed on VFTO Amplitude

The operating speed of disconnecter is an important factor affecting VFTO. For the fast disconnecter, on the one hand, the operation time is short, the number of gap breakdown is less, and the probability of VFTO is low; on the other hand, the residual voltage on the bus after opening is higher, which is not conducive to reducing the VFTO in the closing process. Based on the dynamic arcing model mentioned above, this article takes the opening process as an example to study the influence of the operating speed of disconnecter on VFTO amplitude [14].

During the opening operation, the distance between the moving and static contacts of the disconnecter increases gradually until it reaches the maximum opening distance of the contact gap, so the maximum value of VFTO usually appears in the later stage of a switch operation. When the distance between contacts increases, it is still considered that the positive breakdown voltage is proportional to the time. When the distance between contacts reaches the maximum, the breakdown voltage remains unchanged. Under the premise of considering the restriking arc model, the VFTO amplitude at the end of the branch bus is calculated, respectively, when the opening speed is in the range of 0.1–1.0 m/s, and the results are shown in Table I.

It can be seen from Table I that when the opening speed is less than 0.7 m/s, the VFTO amplitude at the end of the branch bus increases with the increase of the operating speed of the disconnecter. When the opening speed is equal to 0.7 m/s, the VFTO amplitude at the end of the branch bus reaches the maximum. After that, the amplitude of VFTO will decrease with the further increase of opening speed. The above conclusions are basically consistent with the experimental results in the literature [12], which also verifies the correctness of the model built in this article. On the other hand, the repetition of the above simulation results to the existing experimental conclusions makes it possible to study the influence of disconnecter operating speed on VFTO amplitude through the simulation method in this article under the limited experimental conditions. Fig. 10 shows the VFTO waveform at the end of the branch bus when the opening speeds are 0.1 m/s and 0.7 m/s, respectively. It can be found that the faster the opening speed of the disconnecter is, the fewer times of breakdown in an opening process will be.

In the follow-up engineering application, the influence of operating speed on VFTO shall be taken into account in the

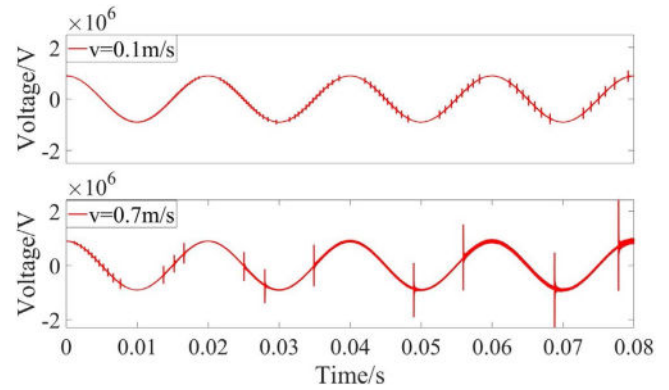


Fig. 10. VFTO waveform at the end of the branch bus when the disconnecting speed of the isolating switch is 0.1 and 0.7 m/s.

selection of disconnecter. The change curve of VFTO amplitude under different disconnecter operating speeds can be obtained through simulation analysis, and the action speed corresponding to the maximum point of the curve can be found. During the selection, the disconnecter corresponding to the critical action speed and its adjacent range shall be avoided to minimize the VFTO amplitude.

VI. CONCLUSION

The accuracy of VFTO simulation in GIS station is largely determined by the accuracy of switch arc simulation. Based on the existing arc analysis theory, a model was established in ATP-EMTP. The arc channel damping was simulated by a series circuit of the resistor and time-varying inductance, the arc striking was modeled based on gaseous dielectric theory, and the arc extinguishing criterion was programmed by energy balance theory. Combined with a 1000 kV GIS test circuit, the dynamic arcing model was simulated, and the influence of operating speed of disconnecter on VFTO during the opening process was studied. According to the simulation results, the following conclusions can be drawn.

- 1) During the opening and closing process, the contact gap voltage difference curve has a power-frequency sinusoidal voltage profile as a whole, and the envelope of the contact gap voltage difference curve is the breakdown voltage curve. At the same time, during the opening process, as the distance of the contact gap increases, the load-side voltage waveform presents a transition from a sine wave to a step wave. The closing process is just the opposite.
- 2) The short bus voltage has an approximate step shape and the outline of the sinusoidal voltage waveform of the power frequency power supply. The transition edge of each step corresponds to a breakdown process, and the narrow pulse corresponding to each transition edge is a high-frequency transient process. The starting point of each step falls on the power frequency power supply voltage waveform. The short bus VFTO is actually a superposition of a high-frequency transient on the power frequency power supply voltage.

- 3) From the two perspectives of the VFTO waveform law and the influence of the opening speed on VFTO amplitude, the simulation conclusions are compared with the test results of the existing literature to verify the accuracy of the simulation model.

In general, the above model provides a new modeling method for the simulation calculation of VFTO in the actual GIS station, and the conclusions obtained can be compared with the experimental results of the existing literature. The model has a certain engineering guiding significance.

REFERENCES

- [1] D. C. Moreira, M. V. A. Nunes, D. D. C. Moreira, and D. K. D. Costa, "Analysis of VFTO during the failure of a 550-kV gas-insulated substation," *Electr. Power Syst. Res.*, vol. 189, Dec. 2020, Art. no. 106825, doi: [10.1016/j.epsr.2020.106825](https://doi.org/10.1016/j.epsr.2020.106825).
- [2] M. A. Haseeb and M. J. Thomas, "Disconnecter switching induced transient voltage and radiated fields in a 1100 kV gas insulated substation," *Electr. Power Syst. Res.*, vol. 161, pp. 86–94, Aug. 2018, doi: [10.1016/j.epsr.2018.04.001](https://doi.org/10.1016/j.epsr.2018.04.001).
- [3] CIGRE Working Group D1.03, "Very fast transient overvoltages (VFTO) in gas-insulated UHV substations," CIGRE Technical Brochure 519, Dec. 2012.
- [4] X. Zhang, "The research on the arc model in disconnector switch for VFTO simulation in GIS," (in Chinese), Master thesis, Dept. School Elect. Electron. Eng., North China Electr. Power Univ., Beijing, China, 2010.
- [5] W. Hu and S. Wang, "Modeling and simulation of single-phase grounding arc in power distribution network based on Mayr-Cassie," (in Chinese), *Elect. Eng.*, no. 9, pp. 48–51, 2020, doi: [10.19768/j.cnki.dgjs.2020.09.013](https://doi.org/10.19768/j.cnki.dgjs.2020.09.013).
- [6] S. A. Boggs, F. Y. Chu, N. Fujimoto, A. Krenicky, A. Plessl, and D. Schlicht, "Disconnect switch induced transients and trapped charge in gas-insulated substations," *IEEE Trans. Power App. Syst.*, vol. PAS-101, no. 10, pp. 3593–3602, Oct. 1982, doi: [10.1109/TPAS.1982.317032](https://doi.org/10.1109/TPAS.1982.317032).
- [7] M. Stosur, M. Szweczyk, W. Piasecki, M. Florkowski, and M. Fulczyk, "GIS disconnector switching operation—VFTO study," in *Proc. Modern Electr. Power Syst.*, 2010, pp. 1–5. [Online]. Available: <https://ieeexplore.ieee.org/document/6007222>
- [8] J. Zhang, H. Wang, J. Zhao, Z. Liu, P. Xie, and H. Chen, "Calculation and analysis of multiple restrikes VFTO based on piecewise arc model," (in Chinese), *High Voltage App.*, vol. 52, no. 5, pp. 14–19, May 2016, doi: [10.13296/j.1001-1609.hva.2016.05.003](https://doi.org/10.13296/j.1001-1609.hva.2016.05.003).
- [9] W. Liu, Y. Xu, Y. Liu, L. Lan, P. Zhang, and D. Yang, "Influence of arcing model on the very fast transient overvoltage in 500 kV GIS substation," (in Chinese), *High Voltage App.*, vol. 53, no. 9, pp. 210–214, Sep. 2017, doi: [10.13296/j.1001-1609.hva.2017.09.036](https://doi.org/10.13296/j.1001-1609.hva.2017.09.036).
- [10] D. Liu, "The research of very fast transient overvoltage in GIS," (in Chinese), Master thesis, Dept. School Elect. Electron. Eng., East China Jiaotong Univ., Nanchang, China, 2015.
- [11] W.-D. Liu, L.-S. Wang, W.-J. Chen, M. Dai, Z.-B. Li, and G.-C. Yue, "Investigation of the VFTO related repeated breakdown processes in UHV GIS," (in Chinese), *High Voltage Eng.*, vol. 37, no. 3, pp. 644–650, Mar. 2011, doi: [10.13336/j.1003-6520.hve.2011.03.013](https://doi.org/10.13336/j.1003-6520.hve.2011.03.013).
- [12] S. Yinbiao et al., "Influence of the switching speed of the disconnector on very fast transient overvoltage," *IEEE Trans. Power Del.*, vol. 28, no. 4, pp. 2080–2084, Oct. 2013, doi: [10.1109/TPWRD.2013.2273620](https://doi.org/10.1109/TPWRD.2013.2273620).
- [13] W. Chen et al., "Experimental research on the characteristics of very fast transient overvoltage in ultra high voltage gas insulated switchgear," (in Chinese), *Proc. Chin. Soc. Elect. Eng.*, vol. 31, no. 31, pp. 38–47, Nov. 2011, doi: [10.13334/j.0258-8013.pcsee.2011.31.009](https://doi.org/10.13334/j.0258-8013.pcsee.2011.31.009).
- [14] B. Wan et al., "Considering restriking arc model 1000kV GIS very fast transient overvoltage characteristics and the influence of disconnector speed," in *Proc. IEEE 4th Int. Elect. Energy Conf. (CIEEC)*, May 2021, pp. 1–6, doi: [10.1109/CIEEC50170.2021.9510928](https://doi.org/10.1109/CIEEC50170.2021.9510928).

Yanze Zhang received the B.S. and M.S. degrees in electrical engineering and automation in 2019 and 2021, respectively, from Wuhan University, Wuhan, China, where he is currently working toward the Ph.D. degree.

His research interests include overvoltage and protection of power system.

Xiaoyue Chen received the Ph.D. degree in electrical engineering and automation from Wuhan University, Wuhan, China, in 2016.

She is currently an Associate Researcher with Wuhan University. Her research interests include power system overvoltage and electromagnetic environment of power system.

Han Cui received the B.S. degree in electrical engineering from Sichuan University, Chengdu, China, in 2021. She is currently working toward the M.S. degree in electrical engineering and automation with Wuhan University, Wuhan, China.

Her research interests include overvoltage and insulation coordination.

Junjie Si received the B.S. degree in electrical engineering and automation in 2021 from Wuhan University, Wuhan, China, where he is currently working toward the M.S. degree.

His research interests include overvoltage and insulation coordination.

Zeyu He received the B.S. degree in electrical engineering and automation from Fuzhou University, Fuzhou, Fujian, in 2018, and the M.S. degree in electrical engineering and automation from Wuhan University, Wuhan, China.

He is currently with State Grid Shaoxing Electric Power Supply Company, Shaoxing, China. His research interests include overvoltage and protection of power system.

Baoquan Wan received the B.S. degree from the former Wuhan University of Water Conservancy and Hydropower, Wuhan, China, in 1995, and the M.S. and Ph.D. degrees from Wuhan University, Wuhan, China, in 2004 and 2007, respectively.

He is currently the Deputy Director of the High Voltage Research Institute, China Electric Power Research Institute Co., Ltd., Beijing, China, and the Deputy Director of the State Power Key Laboratory of Power Grid Environmental Protection. He has long been engaged in testing, research, and standardization of power grid electromagnetic environment, electromagnetic compatibility technology, and UHV transmission technology.

Min Dai received the M.S. degree in electrical engineering and automation from Wuhan University, Wuhan, China, in 2010.

He is currently a Senior Engineer with China Electric Power Research Institute, Beijing, China. His currently major field of interests is electric power system with lightning protection against overvoltage technology and insulation coordination.

Lei Wang received the M.S. degree in electrical engineering and automation from Wuhan University, Wuhan, China, in 2010.

He is a Senior Engineer. He is mainly engaged in lightning protection calculation of substation, overvoltage, and insulation coordination, as well as VFTO test and simulation research.

Jianben Liu received the Ph.D. degree in electrical and electronic engineering from Huazhong University of Science and Technology, Wuhan, China, in 2013.

He is a Senior Engineer. He is mainly engaged in the research and testing of power electronic technology, power quality of power system, and electromagnetic environment of power grid.